Shrinking of hollow Cu_2O and NiO nanoparticles at high temperatures

doi: 10.1016/j.actamat.2008.07.004

Shrinking of hollow Cu_2O and NiO nanoparticles at high temperatures

R. Nakamura[1]*, D. Tokozakura[1], J.-G. Lee[2], H. Mori[3], H. Nakajima[1]

[1]*The Institute of Scientific and Industrial Research, Osaka University, Mihogaoka 8-1, Ibaraki, Osaka 567-0047, Japan*

[2]*Korea Institute of Materials Science, 66 Sangnam-dong, Changwon 641-010, Korea*

[3]*Research Center for Ultra-High Voltage Electron Microscopy, Osaka University, Mihogaoka 7-1, Ibaraki, Osaka 567-0047, Japan*

*Corresponding author: rnakamur@sanken.osaka-u.ac.jp

Abstract

The structural stability of hollow Cu_2O and NiO nanoparticles associated with reduction and oxidation reactions at high temperatures was studied by transmission electron microscopy (TEM). Hollow Cu_2O and NiO in annealing under 5.0×10^{-5} Pa was observed to have shrunk at 473 and 623 K, respectively, where the reduction reactions from oxides to metals started. As a result of shrinking associated with reduction, hollow oxides turned into solid metal nanoparticles after annealing at higher temperatures for a long time. In addition, hollow oxides shrunk and collapsed through high-temperature oxidation. It was found that shrinking of hollow oxides during oxidation occurs at temperature where the diffusion coefficients of slower diffusing species reach around 10^{-22} m^2s^{-1}. Annealing at high temperatures both in a vacuum and in air leads to atomic movement that results in the annihilation of nano-holes inside hollow nanoparticles, and a consequent reduction in e the extra inner-surface energy.

1. Introduction

The synthesis and fabrication of nano-scale controlled materials are rapidly developing fields of materials science [1]. Particularly, hollow nanostructures have attracted much attention because their unique shape makes them applicable as delivery vehicles, fillers as well as for catalysis, and could bring about changes in physical and chemical properties [2,3]. Chemical reaction processes are the most common of the methods to synthesize hollow nanoparticles [4-7]. However, a different principle to fabricate hollow nanoparticles based on the Kirkendall effect was demonstrated by Yin *et al*. [8,9]: the initial solid nanocrystals turn into hollow spheres of cobalt sulfides and oxides when isolated nanocrystals of cobalt are exposed to sulfur and oxygen at relatively low temperatures near 400 K. Thereafter, it was reported by present authors that hollow Zn-[10], Al-[11], Cu-[11,12] and Ni- [13] oxides are formed using metal oxidation reactions. Up to now, it has been commonly recognized that the rapid outward diffusion of metal ions from the metal core to the outer oxide shell during oxidation or sulfidation is accompanied by the generation of vacancies and finally a nano-hole is formed in the oxide particles.

According to several theoretical calculations [14-17], hollow nanospheres are thermodynamically unstable; they tend to shrink into solid nanospheres because a solid nanosphere has a lower surface energy than a hollow nanosphere and is therefore more energetically favorable. However, no experimental studies on structural stability of hollow nanoparticles associated with heat treatment have been performed so far.

In this study, the structural stability of hollow Cu_2O and NiO nanoparticles at high temperatures has been investigated since it is possible to obtain hollow Cu_2O [11,12] and NiO [13] with uniform size distribution by oxidizing Cu and Ni nanoparticles at around 400 K and

700 K, respectively. Compositional change as well as phase transformation associated with annealing was taken into consideration in order to characterize the stability of metal oxides; it is likely that reduction from oxides to metals or phase transformation of oxides with different compositions and crystal structures will occur depending on temperature and atmosphere [18].

The purpose of the present study is to characterize the structural stability of hollow oxide nanoparticles during reduction and oxidation reactions at high temperatures by transmission electron microscopy (TEM).

2. Experimental procedure

Cu nanoparticles were prepared using a Hitachi H-800 type 200 kV TEM equipped with an evaporator in the specimen chamber. A spiral-shaped tungsten filament was used as the evaporator of Cu. An amorphous carbon or alumina film mounted on a Pt or Mo grid with ϕ 3mm for TEM observation was chosen as a substrate supporting the Cu nanoparticles. The substrate was baked out at 800 K for 600 s prior to evaporation. By resistively heating the evaporator, Cu (99.99%) was evaporated from the filament and deposited onto the supporting film under a base pressure around 5×10^{-5} Pa. The temperature of the supporting film during the evaporation was set at 673~873 K in order to obtain nanoparticles of a specific diameter (d = 10~40 nm). The nanoparticles on the substrate were subjected to 423 K for 3.6~7.2 ks in air on the TEM sample holder and then hollow Cu_2O nanoparticles were obtained [11,12].

Ni nanoparticles were prepared by electron-beam deposition in a high-vacuum chamber with a base pressure of approximately 1×10^{-5} Pa. An amorphous Al-oxide film on a Pt grid was used as the supporting film (substrate) for the Ni nanoparticles. A quartz thickness monitor was attached between the source and the substrate in order to control the deposition rate and average

thickness. The substrate was baked at 1000 K for 600 s prior to evaporation. Ni nanoparticles were evaporated onto the substrate kept at 900~950 K with a rate of 0.05-0.10 nmmin^{-1}. By annealing the Ni nanoparticles on the substrate in an electric furnace at 673 K for 3.6 ks in air [13], we obtained hollow NiO nanoparticles.

The hollow Cu_2O and NiO nanoparticles were annealed at higher temperatures in a vacuum and in air, respectively. The isochronal annealing of the hollow Cu_2O and NiO from 423 to 873 K at intervals of 50 K and 1.8 or 3.6 ks in a vacuum was performed in the TEM under 5×10^{-5} Pa and the changes in morphology and structure of them were observed in-situ. To avoid the possible oxide-reduction induced by electron beam in operating, the beam was irradiated only when taking the images. On the other hand, the hollow oxide nanoparticles mounted on the substrate were annealed from 523 to 773 K for Cu_2O and from 873 to 923K for NiO for a given time in an electric furnace controlled within ±0.5 K in air. Changes in morphology and crystal structure after oxidation were observed by the TEM.

3. Results and discussion

3.1. Annealing in vacuum

3.1.1. Cu_2O

Figures 1(a) and (b) show bright field images (BFIs) of hollow Cu_2O nanoparticles during isochronal annealing in TEM from 423 to 573 K for 3.6 ks and their corresponding selected area electron diffraction (SAED) patterns. The diameter of the hollow Cu_2O nanoparticles before the annealing was (a) 10-20 nm and (b) 40-50 nm, respectively. After annealing at 423 K for 3.6 ks , no change in morphology can be seen (Fig. 1(a)). It is obvious, however, that hollow Cu_2O starts to shrink after annealing at 473 K for 3.6ks (Figs. 1(a) and (b)). As the annealing temperature increases, the shrinking of hollow Cu_2O particles proceeds and the nano-holes

inside particles become smaller. Finally, the solid nanoparticles are formed after annealing at 523 K (Figs. 1(a)) and 573 K (Figs. 1(b)), respectively.

The change in the electron diffraction patterns can be seen after annealing at 473 K; hence the ring for the Cu (200) plane appears both in Figs. 1 (a) and (b). The line profiles of the corresponding SAED patterns of Figs. 1(a) and (b), which were converted by using the free software “Process Diffraction” developed by Läbär [19], are indicated in Figs. 2 (a) and (b), respectively. The lower profile at the bottom of each graph is the reference for face-centered cubic(fcc) Cu. The line profile after annealing at 423 K for 3.6 ks of Fig. 2(a) is consistent with the reference line of Cu_2O. However, the small peak corresponding to (200) plane of fcc Cu appears at 473 K for 3.6 ks in Figs. 2 (a) and (b), suggesting that the reduction of Cu_2O starts at that temperature and that the starting temperature doesn’t depend on the diameter of the hollow nanoparticles. The peaks for Cu_2O don’t completely disappear after annealing at 573 K for 60min, although they become weaker with increasing annealing temperature. This result indicates that Cu_2O clusters remain inside Cu nanoparticles. It seems that annealing for a longer time or at a higher temperature is necessary for the complete removal of oxygen from the reduced nanoparticles. A similar behavior has been observed in the reduction of Cu_2O nanopowders with H_2. [20]

Figure 3 shows the reduction behavior of Cu nanoparticles surrounded by Cu_2O layers with about 8 nm in thickness. Although the thickness of Cu_2O layers does not change after annealing at 423 K, it begins to decrease at 473 K. The Cu_2O layers cannot be seen after annealing at 523 K. It is evident that the reduction reaction begins at 473 K because the intensity of Cu_2O starts to decrease and the intensity of fcc Cu increase at 473 K, as can be seen in the line profile of Fig. 4. For example, the intensity of the Cu_2O (111) plane becomes weaker and the shoulder peaks, such as (200), (211) and (222), disappear at 473 K. The starting temperature of reduction of a

thin Cu_2O film for Cu/Cu_2O is consistent with that for hollow Cu_2O, indicating that the structure of particles doesn't affect the reduction reaction.

When the Cu nanoparticles reduced from hollow Cu_2O particles were re-oxidized at 423 K for 3.6 ks in air, hollow Cu_2O were confirmed to have been formed again. Then, the hollow Cu_2O turned into solid Cu nanoparticles after annealing in a vacuum. Therefore, the changes in morphology and crystal structure through the oxidation of Cu nanoparticles and the reduction of hollow Cu_2O can reversibly take place. In Fig. 5, a typical example of changes in morphology of hollow Cu_2O nanoparticles in the 3rd cycle of reduction and oxidation. After annealing hollow Cu_2O nanoparticles at 573 K for 1.8 ks under 5×10^{-5} Pa (Fig. 5(a)), a spherical particle was observed to have formed along the inner surface of hollow particles, as indicated by arrows. This behavior suggests strongly that reduced Cu atoms are generated at the inner surface of hollow Cu_2O and they aggregate via surface diffusion. Figure 5(b) shows a BFI of Cu nanoparticles, which were fully reduced from hollow Cu_2O after the third cycle of annealing of hollow Cu_2O at 773 K for 1.8 ks in a vacuum. As indicated by arrows, the brighter areas of an amorphous-carbon supporting film can be seen in the vicinity of the Cu nanoparticles. It seems likely that these areas represent the original positions of as-evaporated Cu nanoparticles. If hollow Cu_2O nanoparticles shrunk uniformly to be solid Cu nanoparticles as a result of reduction, the position of the particles on a supporting film after the cycle of oxidation and reduction would remain unchanged. However, Cu particles were observed to have formed at the off-centered position of hollow Cu_2O in the course of the reduction reaction, as shown in Fig. 5(a). The localization of Cu nanoparticles causes the shift of the particles from the original position of as-evaporated Cu nanoparticles after the reduction reaction. Formation of Cu nanoparticles along the inner surface of hollow Cu_2O during reduction of Cu_2O to Cu provides an important clue to consider the mechanism of mass transport in shrinking.

3.1.2. NiO

Figure 6 shows the change in morphology of hollow NiO during isochronal annealing from 573 to 873 K under vacuum in TEM. Hollow structures of NiO nanoparticles remain after annealing at 573 K for 1.8 ks, but it can be seen that hollow NiO nanoparticles start to shrink at 623 K for 1.8 ks. The shrinking of nano-holes in hollow NiO proceeds with increasing temperature and all the hollow nanoparticles turn into solid spheres after annealing at 873 K. The electron diffraction patterns after annealing at 573 K is the same as that before annealing. However, the ring of Ni (200) plane appears at 623 K where shrinking of hollow NiO starts. The starting temperature for shrinking accords with that of the reduction from NiO to Ni, indicating that shrinking of hollow NiO is closely related to the mass transport during the reduction reaction.

Figure 7 shows a BFI of hollow NiO after annealing it in vacuum at 773 K for 1.8 ks. The shrinking behavior of hollow NiO is similar to that of hollow Cu_2O; nanoparticles are formed along the inner surface of hollow NiO spheres.

3.1.3. Shrinking mechanism during reduction

According to the kinetic models of reduction of oxides [21], oxygen ions are removed from the lattice of the surface leaving behind an anion vacancy and then reduced zone are formed on the surface at the initial stage of reduction. In general, a dominant process of reduction reaction is considered to be the outward diffusion of oxygen ions via the anion vacancies generated at the surface [22]. Such mass transport results in the inward movement of the metal/reduced oxide interface. This is true of the reduction of hollow oxides; oxygen ions are removed from the outer surface to vacuum. As mentioned earlier, however, the formation of metal

nanoparticles along the inner surface of hollow oxides during the reduction of Cu_2O to Cu (Fig. 5(a)) and NiO to Ni (Fig. 7), respectively, demonstrates that the reduced Cu and Ni atoms are generated at the inner surface of hollow Cu_2O and NiO. The formation of metal nanoparticles at the inner surface indicates that oxygen ions diffuse from the inner surface migrate to the outer surface and that the reduced zone (i.e. Cu and Ni layers) is formed at the inner surface. After the formation of metal layers, metal atoms aggregate and make a particle in order to fill in the nano-hole. This behavior can be interpreted as the self-assembly of metal atoms which causes the extra energy of the inner surface of a hollow sphere to lower. It takes so long for the complete removal of oxygen that metal atoms at the inner surface have enough time to diffuse and aggregate by surface diffusion along the inner surface, resulting in the formation of metal particles inside oxide shell as shown in Fig. 5(a) and Fig. 7.

3.2. Annealing in air

3.2.1. Cu_2O

Figure 8 shows BFIs of hollow Cu_2O nanoparticles (a) before and after oxidation at 573 K in air for (b) 3.6, (c) 36 and (d) 3.6×10^2 ks and their corresponding SAED patterns (a')-(d'). The hollow structures remain after the oxidation at 573 K for 3.6 ks. However, the diffraction patterns corresponding to Cu_2O disappear and those to CuO appear in the SAED of Fig. 8(b'); the phase transformation from Cu_2O to CuO occurs at 573 K. The result that Cu_2O transform to CuO at 573 K in air is in accordance with that obtained by Li *et al.*[18], who studied the oxidation of Cu_2O thin films by both TEM and X-ray diffractometry. The shell thickness of hollow CuO is almost consistent with that of hollow Cu_2O. When CuO is formed through the oxidation reaction, $Cu_2O+1/2O_2 \rightarrow 2CuO$, the volume expansion from Cu_2O to CuO is about

110%, taking into account the density and mass change. The volume expansion is so small that the shell thickness hardly changes before and after the formation of hollow CuO. After the long-time oxidation at 573 K for 36 and 360 ks, the hollow shape and the crystal structure of CuO don't change. The diffraction rings of (c') and (d') become clearer and sharper compared to those of (b'), indicating that the crystallinity of CuO becomes more definite because of the long-time annealing. By oxidizing Cu nanoparticles at 573 K, it is possible to obtain hollow CuO nanoparticles which are thermally stable in structure even after long-time annealing at the temperature.

The change of morphology at higher temperature can be seen in Fig. 9, where a BFI of hollow Cu_2O nanoparticles oxidized at 673 K for 1.2 ks is shown. The inner pores of CuO hollow nanoparticles were observed to be filled uniformly from the inner surface, suggesting that hollow CuO starts to shrink at this temperature. It should be noted that the shrinking behavior in the oxidation of CuO hollow spheres is different from that in the reduction of Cu_2O to Cu shown in Fig. 5(a), where the spherical Cu particles were observed to be formed along the inner surface of hollow Cu_2O.

In Fig. 10, a BFI of hollow Cu_2O nanoparticles after oxidation at 773 K for 3.6 ks and the corresponding SAED patterns are shown. As can be seen in the figure, hollow nanoparticles turn completely into solid structures with the crystal structure of CuO being maintained.

3.2.2. NiO

The shrinking of hollow NiO nanoparticles was also observed when they were oxidized at higher temperatures. Figure 11 shows the change in morphology of hollow NiO through oxidation at higher temperatures from 873 to 923 K in air and their corresponding SAED patterns. Although hollow structures are maintained after oxidation at 873 K for 36 ks and 923

K for 3.6 ks, almost all hollow particles collapse into solid spheres at 923 K for 36 ks. Unlike the oxidation of Cu_2O, no transformation was observed during the oxidation of NiO in air.

3.2.3. Mechanism of shrinking during oxidation

According to the theoretical consideration on the shrinking of hollow binary alloy nanoparticles [15], the rate of shrinking is controlled by the slower diffusing specie of the alloy. This idea can be applied to the discussion on shrinking of hollow CuO and NiO through the oxidation above 673 and 923 K since shrinking by oxidation doesn't accompany phase transformation, unlike the shrinking by reduction which occurs with the phase transformation from an oxide to a metal.

Atkinson and Taylor reported that the activation energy and pre-exponential factor for the self-diffusion of Ni in NiO are 245 $kJmol^{-1}$ and 2.2×10^{-6} m^2s^{-1}, respectively [22]. O'Keeffe and Moore determined those of O in NiO to be 226 $kJmol^{-1}$ and 1×10^{-9} m^2s^{-1}, respectively [23]. At 923 K, where hollow NiO nanoparticles completely collapse, the self-diffusion coefficient of Ni and O in NiO are estimated to be 3×10^{-20} m^2s^{-1} and 1.6×10^{-22} m^2s^{-1}, respectively, based on the Arrhenius equation. On the other hand, the self-diffusion coefficients of Cu [24] and O [25] in CuO at 673 K, where hollow CuO nanoparticles shrink, are 1.3×10^{-22} m^2s^{-1} and 3×10^{-16} m^2s^{-1}, respectively. It is found that the diffusion coefficients of the slower diffusing species, O in NiO and Cu in CuO, at the temperature where shrinking of hollow oxides takes place, are around 10^{-22} m^2s^{-1}. When D is 10^{-22} m^2s^{-1} and t is 3.6 ks, the average diffusion distance, $\sqrt{Dt}$, is estimated to be of the order of 0.1 to 1 nm, which is smaller than 10 to 20 nm corresponding to the radius of hollow oxide nanoparticles. It seems that, however, the calculated value can be close to several to ten nanometers, though it must be remembered that it was calculated by using the Arrhenius parameters obtained from the diffusion coefficients at high temperatures.

Therefore, it is expected that atomic diffusion to fill in the nano-hole with several to ten nanometers in diameter can occur at temperatures where the diffusion coefficient is around 10^{-22} m^2s^{-1}. It seems that this result supports the idea by Gusak *et al*. [15] that the rate of shrinking is controlled by the slower diffusing specie is valid. It should be noted that shrinking of hollow oxides by high-temperature oxidation starts at a temperature where the diffusion coefficient of the slower diffusion species reaches about 10^{-22} m^2s^{-1}.

4. Conclusions

(1) The shrinking of hollow Cu_2O and NiO occurs at 473 and 623 K, respectively, where the reduction reactions from oxides to metals start in annealing them under 5.0×10^{-5} Pa. Hollow Cu_2O and NiO turn into solid Cu and Ni nanoparticles as a result of the shrinking associated with reduction.

(2) The starting temperature of reduction of hollow Cu_2O doesn't depend on the diameter of the hollow nanoparticles. Furthermore, the starting temperature of reduction of a Cu_2O thin film with Cu/Cu_2O structure is consistent with that with hollow Cu_2O, indicating that the structure of particles doesn't affect the reduction reaction

(3) In the course of the reduction reactions, metal nanoparticles are formed along the inner surface of hollow oxides, suggesting that (i) oxygen ions diffuse outward from inner to outer surface, (ii) the reduced Cu layer is formed at the inner surface and (iii) the reduced Cu atoms aggregate to form a nanoparticles by surface diffusion.

(4) Hollow CuO is obtained after oxidizing hollow Cu_2O at 573 K in air and is stable in structure at the temperature in spite of its need for long-time annealing.

(5) Hollow CuO and NiO shrink and collapse to form solid oxide particles at 673 K and 923 K, respectively.

(6) It seems that shrinking of hollow CuO and NiO nanoparticles occurs at temperatures where the diffusion coefficients of slower diffusing ions in the oxides are of the order of 10^{-22} m^2s^{-1}.

Acknowledgements

One of the authors (R. Nakamura) would like to thank Dr. T. Sakata and Mr. E. Taguchi of The Research Centre for Ultra-High Voltage Electron Microscopy, Osaka University for their technical support in the operation of TEM. This work was supported by Grant-in-Aid for Scientific Research (Category S) and also by Priority Assistance for the Formation of World wide Renowned Centers of Research- The Global COE Program (Project: Center of Excellence for Advanced Structural and Functional Materials Design), from the Ministry of Education, Culture, Sports, Science and Technology, Japan.

REFERENCES

[1] Xia Y, Halas NJ. MRS Bulletin 2005;30:356.

[2] Kim SW, Kim M, Lee WY, Hyeon T. J Am Chem Soc 2002;124:7642.

[3] Sun Y, Xia Y. J Am Chem Soc 2004;126:3892.

[4] Lee J, Sohn K, Hyeon T. J Am Chem Soc 2001;123:5146.

[5] Mandal TK, Fleming MS, Walt DR. Chem Mater 2000;12:3481.

[6] Graf C, van Blaaderen A. Langmuir 2002;18:524.

[7] Caruso F, Caruso RA, Möhwald H. Science 1998;282:1111

[8] Yin Y, Rioux RM, Erdonmez CK, Hughes S, Somorjai GA, Alivisatos AP. Science 2004;304:711.

[9] Yin Y, Erdonmez CK, Cabot A, Hughes S, Alivisatos AP. Adv Func Mater 2006;16:1389.

[10] Nakamura R, Lee JG, Tokozakura D, Mori H, Nakajima H. Mater Lett 2007;61:1060.

[11] Nakamura R, Tokozakura D, Nakajima H, Lee JG, Mori H. J Appl Phys 2007;101:074303.

[12] Tokozakura D, Nakamura R, Nakajima H, Lee J-G, Mori H. J Mater Res 2007;22:2930.

[13] Nakamura R, Lee JG, Mori H, Nakajima H. Phil Mag 2008;88:257

[14] Tu KN, Gosele U. Appl Phys Lett 2005;86.

[15] Gusak AM, Zaporozhets TV, Tu KN, Gösele U. Phil Mag 2005;85:4445

[16] Evteev AV, Levchenko EV, Belova IV, Murch GE. Phil Mag 2007;87:3787

[17] Fischer FD, Svoboda J. J Nanoparticle Res 2008;10:255.

[18] Jian L, Vizkelethy G, Revesz P, Mayer JW, Tu KN. J Appl Phys 1991;69:1020.

[19] Labar JL. Ultramicroscopy 2005;103: 237.

[20] Kim JY, Rodriguez JA, Hanson JC, Frenkel AI, Lee PL. J Am Chem Soc 2003;125:10684.

[21] Kung HH, Transition Metal Oxides: Surface Chemistry and Catalysis (Elsevior, Newe York, 1989)

[22] Sholtz JJ, Langell MA. Surf Sci 1985;164:543.

[22] Atkinson A, Taylor RI. Phil Mag A 1979;39:581.

[23] O'Keeffe M, Moore WJ. J Phys Chem 1965;65:1438.

[24] Tu KN, Yeh NC, Park SI, Tsuei CC. Phys Rev B 1989;39:304.

[25] Rebane JA, Yakovlev NV, Chicherin DS, Tretyakov YD, Leonyuk LI, Yakunin VG. J Mater Chem 1997;7:2085.

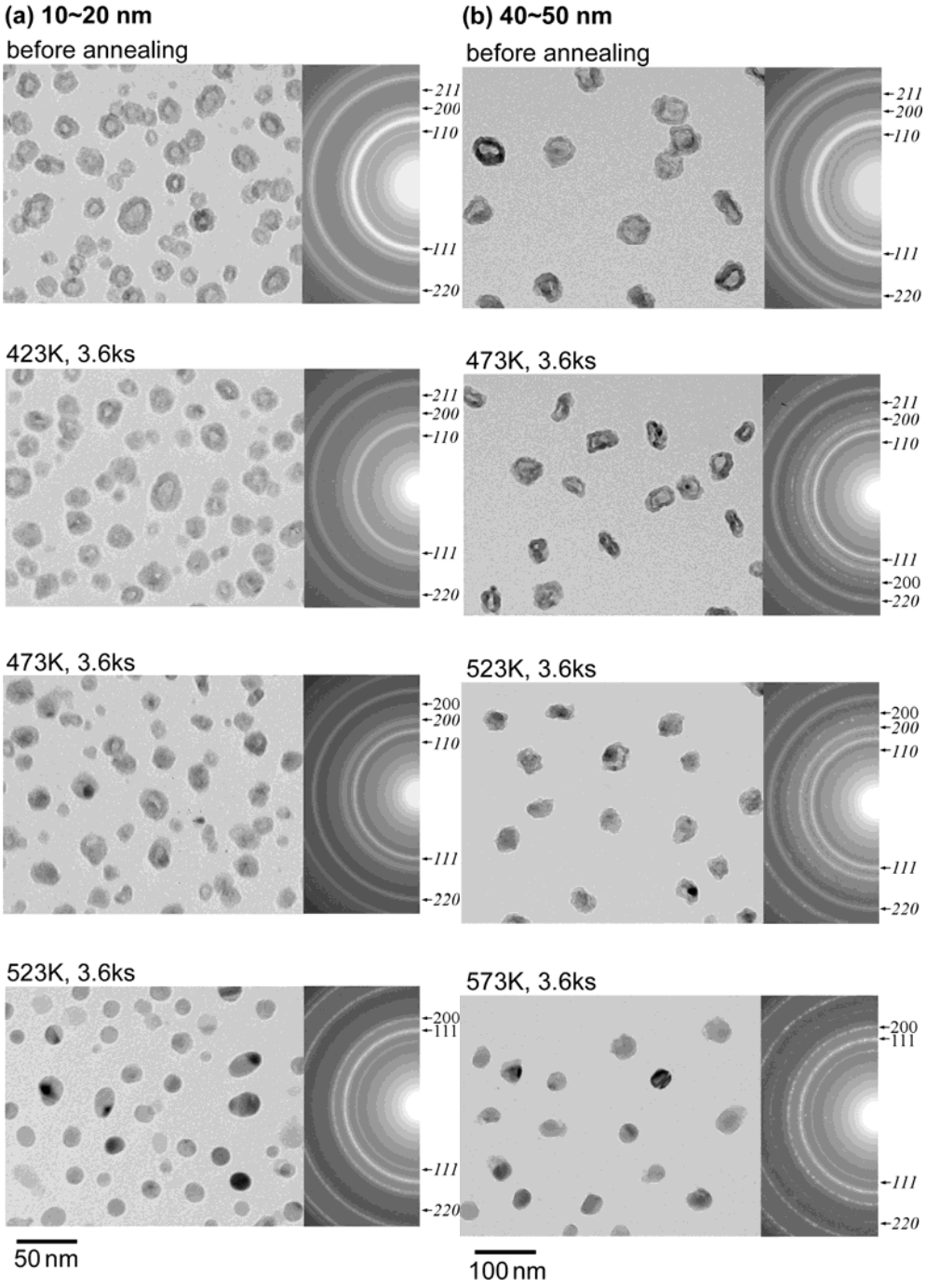

Fig 1. Bright field images of hollow Cu_2O nanoparticles before annealing and during isochronal annealing for 1.8 ks in TEM from 423 to 573 K and their corresponding selected area electron diffraction (SAED) patterns. Initial diameters of hollow Cu_2O nanoparticles are (a) 10~20 nm and (b) 40~50 nm, respectively. Normal and italic numbers represent the plane indexes for Cu and Cu_2O, respectively.

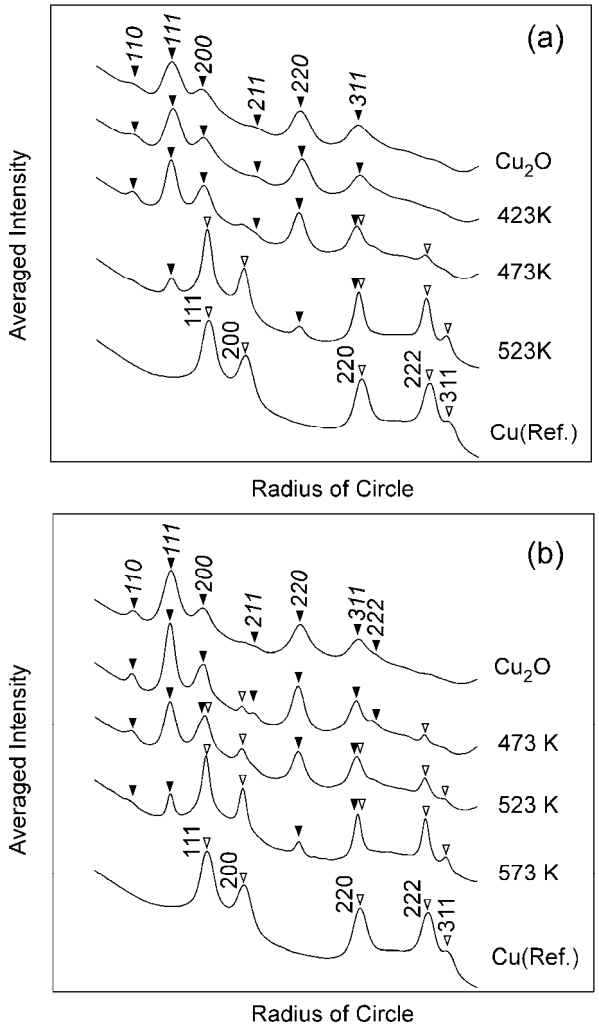

Fig 2. Line profiles of the corresponding SAED patterns shown in Figs. 1(a) and (b), which were converted through the free software “Process Diffraction”. Normal and italic numbers represent the plane indexes for Cu and Cu_2O, respectively.

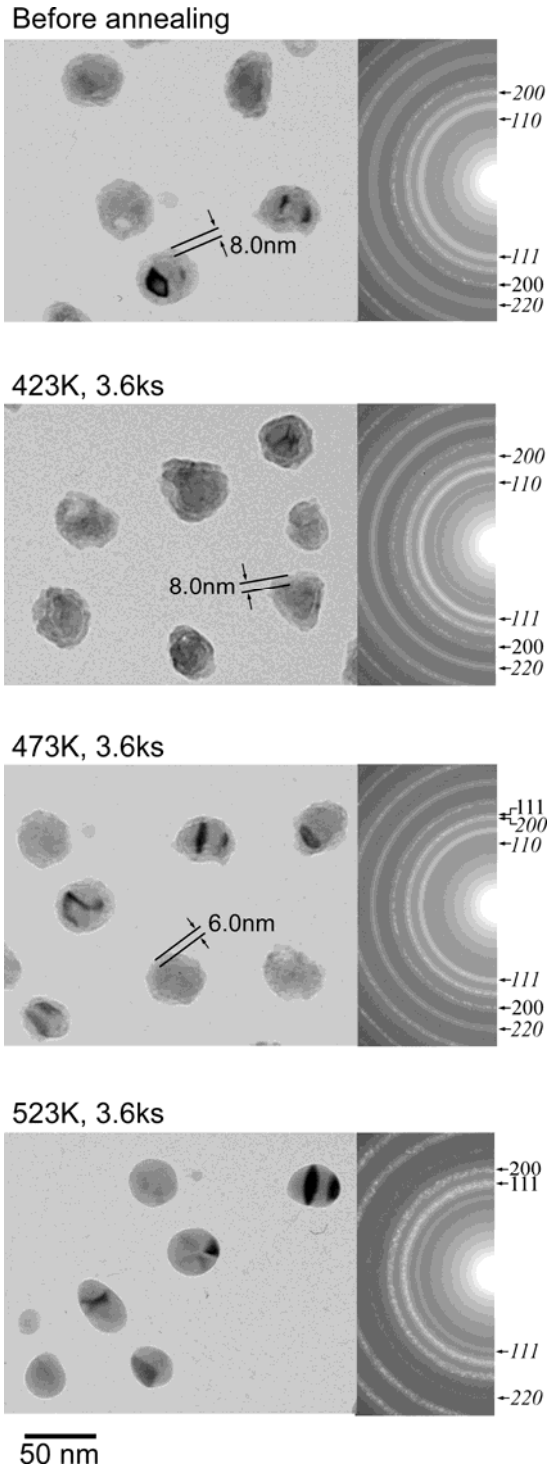

Fig. 3. BFIs of Cu nanoparticles surrounded by a Cu_2O thin film during isochronal annealing in TEM from 423 to 573 K for 3.6 ks and corresponding SAED patterns.

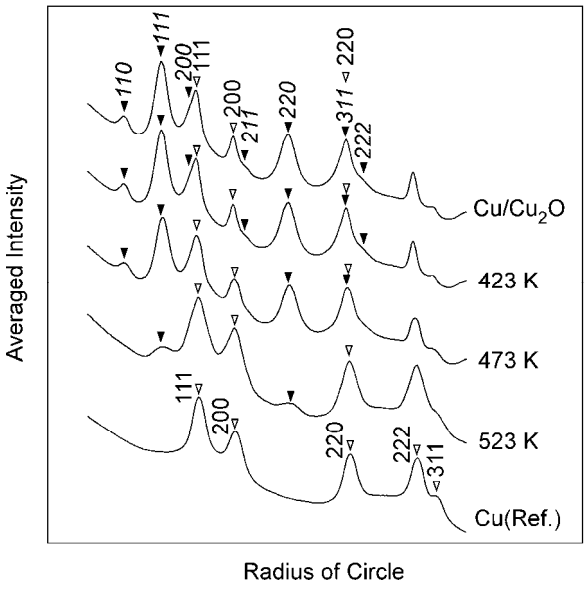

Fig. 4. Line profiles of the corresponding SAED patterns for the annealing of Cu/Cu_2O nanoparticles shown in Fig. 3.

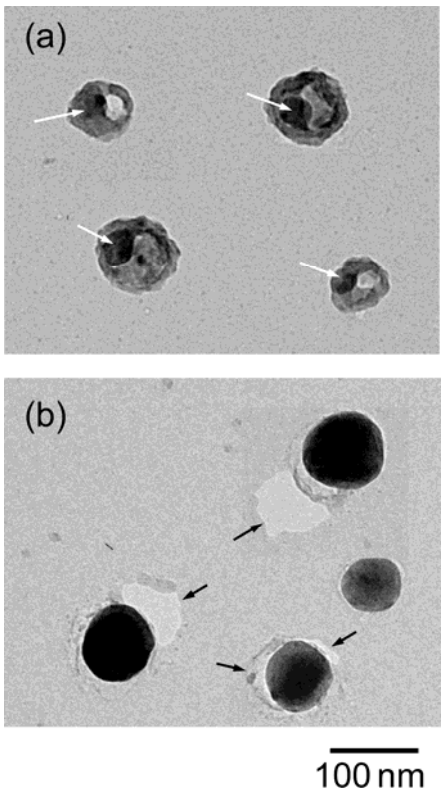

Fig. 5. BFIs of hollow Cu_2O nanoparticles in the 3rd cycle of annealing in TEM after (a) 573 K, 1. 8ks and (b)773 K, 1.8 ks.

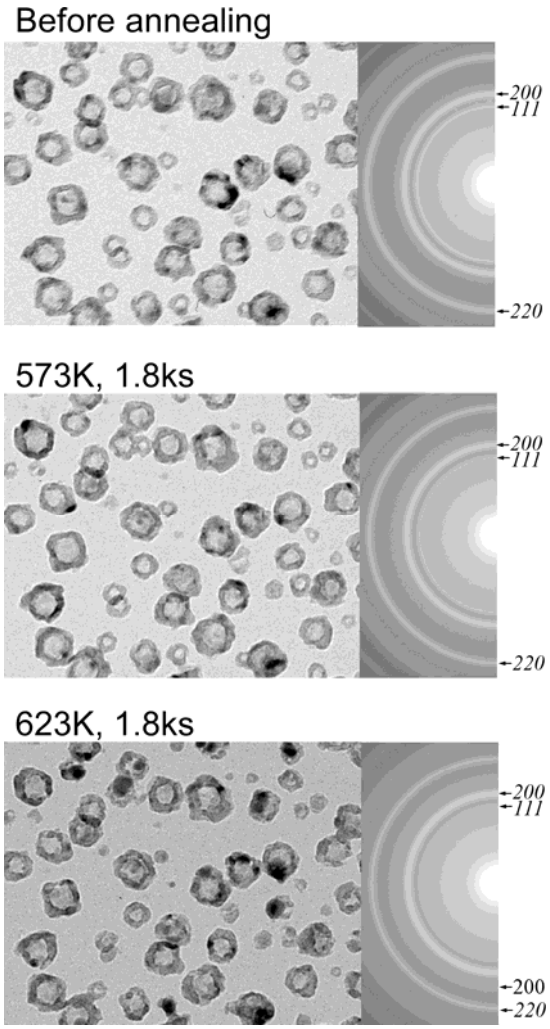

Fig. 6. BFIs of hollow NiO nanoparticles during isochronal annealing for 1.8 ks in TEM from 573 to 873 K and their corresponding SAED patterns. Normal and italic numbers represent the plane indexes for Ni and NiO, respectively.

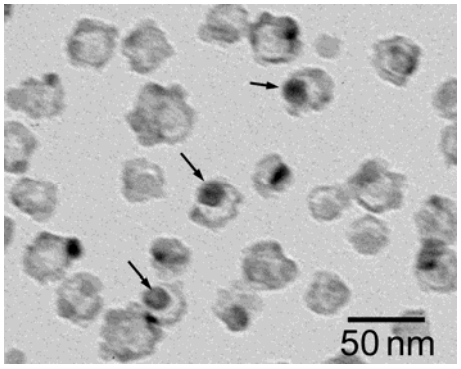

Fig. 7. A typical example of hollow NiO nanoparticles in the course of annealing at 773 K for 1.8 ks.

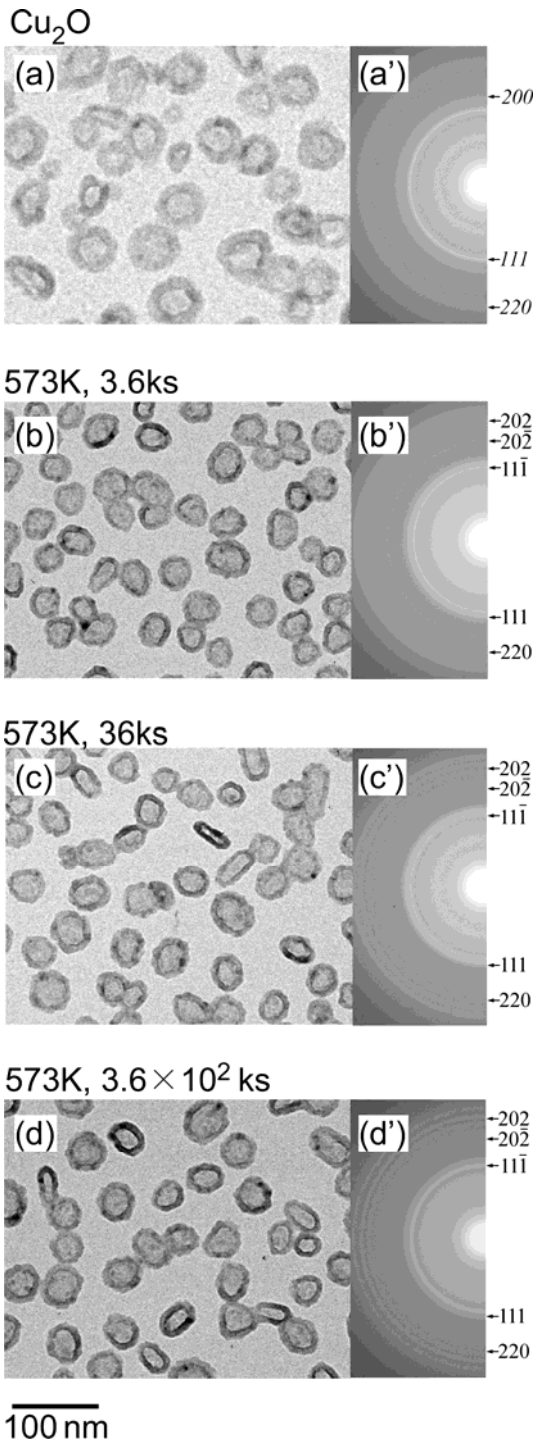

Fig. 8. BFIs of hollow Cu_2O nanoparticles (a) before and after oxidation at 573 K in air for (b)3.6, (c) 36 and (d) 3.6×10^2 ks and their corresponding SAED patterns (a')~(d').

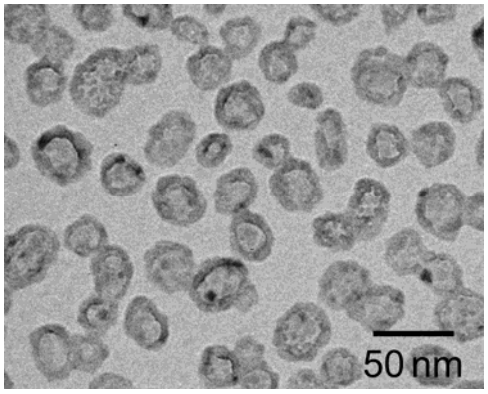

Fig. 9. BFIs of hollow Cu_2O nanoparticles after oxidation at 673 K for 1.2 ks.

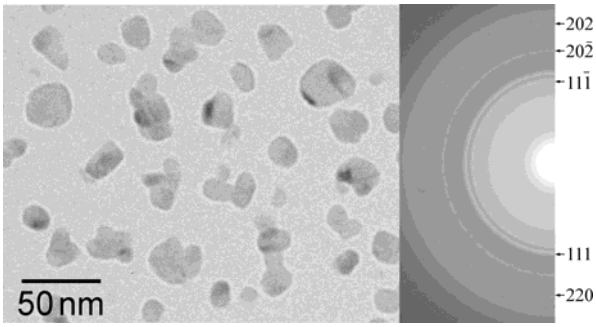

Fig. 10. BFIs of hollow Cu_2O nanoparticles after oxidation at 773 K for 3.6 ks and the corresponding SAED pattern. Numbers indicate the plane indexes for CuO.

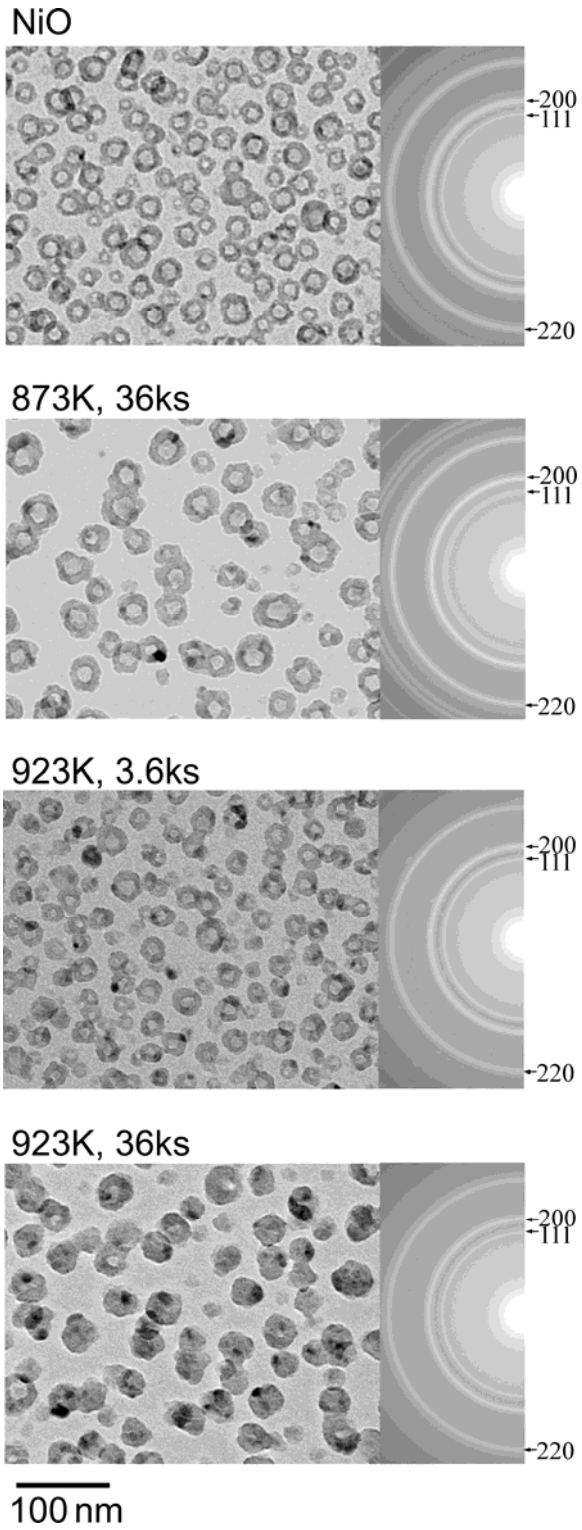

Fig. 11. BFIs of hollow NiO nanoparticles before and after oxidation at 873~923 K and the corresponding SAED patterns. Numbers indicate the plane indexes for NiO.